FUNDAMENTALS & APPLICATIONS

CHEMELECTROCHEM

ANALYSIS & CATALYSIS, BIO & NANO, ENERGY & MORE

Accepted Article

Title: Electrocatalytic oxidation of Glycerol on Pt single crystals in alkaline media

Authors: Regiani Maria Leopoldina Martins Sandrini, Juliane Renata Sempionatto, Germano Tremiliosi-Filho, Enrique Herrero, Juan M Feliu, Janaina Souza-Garcia, and Camilo Andrea Angelucci

To be cited as: *ChemElectroChem* 10.1002/celc.201900311

Link to VoR: http://dx.doi.org/10.1002/celc.201900311

A Journal of

ChemPubSoc Europe

WILEY-VCH

www.chemelectrochem.org

Electrocatalytic oxidation of Glycerol on Pt single crystals in alkaline media.

Regiani M. L. M. Sandrini[1], Juliane R. Sempionatto[2], Germano Tremiliosi-Filho[3], Enrique Herrero[4], Juan M Feliu[4]*, Janaina Souza-Garcia[1], Camilo A. Angelucci[1]*

1 *Federal University of ABC, Center for Natural and Human Sciences, Av. dos Estados, 5001, 09210-580, Santo André-SP, Brazil*

2 *Department of NanoEngineering, University of California, San Diego, La Jolla, California 92093, United States*

3 *Institute of Chemistry of São Carlos, University of São Paulo, P.O. Box 780, 13560-970 São Carlos, São Paulo, Brazil*

4 *Instituto de Eletroquímica, Universidad de Alicante, Apdo. 99, E-03080, Alicante, Spain*

10.1002/celc.201900311

TABLE OF CONTENT

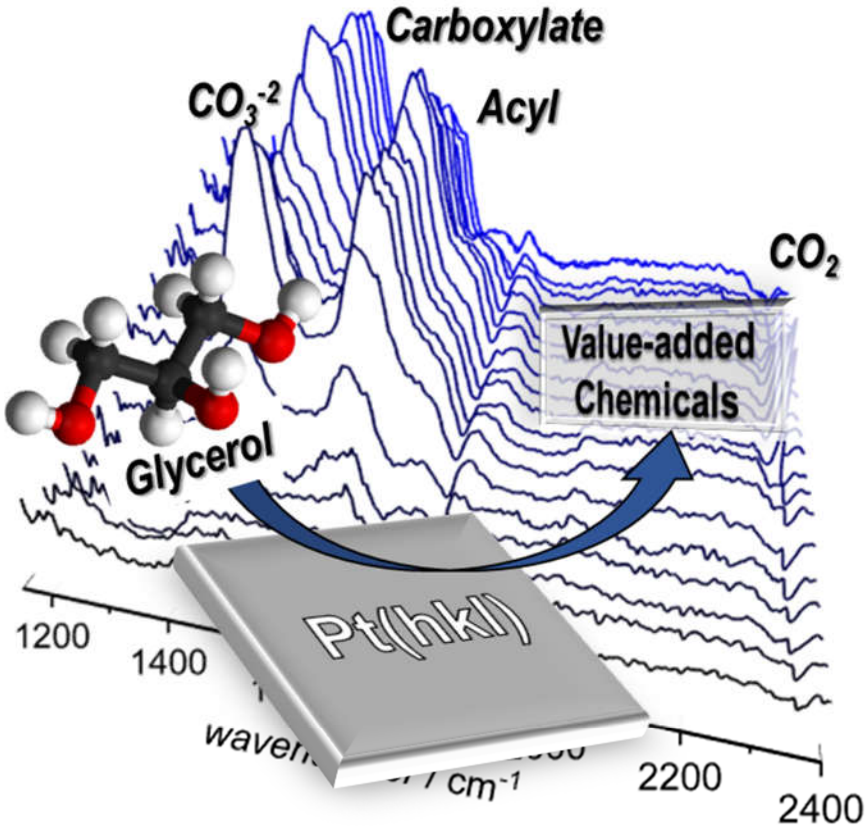

Glycerol electrooxidation on Pt single crystal electrodes is a strongly structure sensitive reaction. In alkaline media the electrode activity is highly suppressed with subsequent potentiodynamic cycles. The Pt(100) electrode has shown to be less prone to poisoning in contrast to Pt(110) and Pt(111). In-situ FTIR results show the rate of deactivation is also related to the electrode surface suggesting the mechanism undergoes through glycerol dehydrogenation to alkoxydes, followed by formation of aldehyde intermediates adsorbed as η^1(O)-aldehyde and η^1(C)-acyl geometry

Abstract

Glycerol adsorption and oxidation reactivity at platinum single crystal electrodes in alkaline media using electrochemical and Fourier transform infrared (FTIR) techniques are reported. The behavior of Pt(100) and Pt(110) for the glycerol electrooxidation reaction (GEOR) were compared and analyzed altogether with those previously reported for Pt(111).(R. M. L. M. Sandrini, J. R. Sempionatto, E. Herrero, J. M. Feliu, J. Souza-Garcia, C. A. Angelucci, *Electrochem. commun.* **2018**, *86*, 149–152*)* The voltammetric profiles confirm the structure sensitivity of GEOR as well as the role of the surface atoms orientation on the electrocatalytic activity. The Pt(100) surface has shown to be less prone to poisoning during multiple potential cycles in contrast to Pt(110) which suffers an accentuate deactivation at the first positive-going scan. Spectroscopic results show that the GEOR on all three surfaces is characterized by the presence of two broad bands, centered circa 1400 cm^{-1} and 1600 cm^{-1}. This provides evidence that GEOR mechanism undergoes, through glycerol dehydrogenation, to alkoxydes followed by formation of aldehyde intermediates adsorbed as η^1(O)-aldehyde and η^1(C)-acyl geometry, respectively. The surface atomic arrangement induces different selectivity in the oxidation process.

Keywords: *Glycerol, oxidation, in situ FTIR, Alkaline media, platinum, single-crystal.*

1- Introduction

The glycerol (GlyOH) molecule has become in the past decades a key raw material due to its low price and high availability.[1] Obtained as a co-product from Biodiesel production via transesterification of vegetable oils or animal fats, the biodiesel-generated glycerol has followed the rapid expansion of biodiesel industry due to the environmental policies demands that seeks for alternatives of petro-fuels dependency.[2] However, unlike the biodiesel, the current market was unable to absorb the surplus of glycerol, resulting in a low price and problems in distributing the substance excess. Then, the conversion of glycerol into value-added products presents a potential opportunity to the biodiesel industry finds new markets or new applications.[3]

From the molecular point of view glycerol is a very versatile and highly functionalized molecule. With three vicinal alcoholic groups they can act as reaction centers resulting the

basis to generate a large variety of derivatives.[4] In this scenario the electrosynthetic pathway, through the use of electrocatalysts, has proved one of the alternatives to selectively oxidize glycerol under mild condition and greener approaches in various high value compounds such as dihydroxyacetone, glyceraldehyde, glyceric acid, hydroxypyruvic acid, among others.[5–8]

As any other electrosynthetic reaction, the selectivity of the electrooxidation of glycerol reaction (GEOR) depends on many experimental parameters including the nature of the catalyst. Various metallic and bimetallic electrocatalysts has shown to be active to oxidize glycerol.[5,9–11] Recently, Pt-based nanostructured catalysts have shown superior electroactivity and selectivity when combined with other metals as Cu,[12,13] Au,[14] among others.[15]

Platinum is of particular interest due to its versatility to oxidize small organic molecules in a wide pH range at high reaction rates. In fact, during the last few years a substantial number of investigations have devoted to understand the GEOR on platinum catalyst.

Kwon *et al.*[8] using high-performance liquid chromatography analyzed the soluble products produced during the GEOR on Pt electrode. They showed a potential dependency on products formation with glyceraldehyde been formed at low potentials serving as the reactive intermediate to produce glyceric acid, and then to glycolic acid and formic acid as the potential was made more positive. Dihydroxyacetone and hydroxypyruvic acid were also detected, but at low concentrations.

Schnaidt et. al.[16] applied a combined spectroelectrochemical DEMS/ATR-FTIRS set-up to study the glycerol adsorption/oxidation mechanism on Pt catalyst in acidic media. The authors detected carbon monoxide, glycerol and glycerate adsorbed on Pt surface, and glyceric acid as soluble product.

In fact, the diversity of products formed from GEOR has intrinsic relation to the interaction of reactive intermediate, spectators, solvent and electrolyte with the metal surface. Such interaction is a consequence of both the nature of the adsorbate and the nature of the surface. Accordingly, the crystallographic orientation of the atoms on the catalyst surface plays a key role in electrocatalysis, as well as in organic electrosynthesis. The use of well-ordered single crystal electrodes as model surfaces has provided an indispensable strategy when one wants to study specific reaction parameters in isolation. Despite the advantages of using single crystals to gather deeper insights about the kinetics and mechanism reaction, the impact of structure sensitivity of GEOR is a scarcely investigated issue. [17–22]

In a recent study, Garcia *et al.*[17] showed that, besides the structure-sensitive process, the GEOR in acidic media selectively oxidize glycerol to glyceraldehyde, glyceric acid, and dihydroxyacetone on Pt(111) while only glyceraldehyde was detected as the main product of the reaction on the Pt(100) electrode.

Studying the GEOR on Pt basal plane electrodes Gomes and co-workers[21] showed that Pt(111) is less prone to catalyze the scission of C-C bond, while on Pt(110) and Pt(100) revealed the formation of adsorbed CO (CO_{ads}) at potential as low as 0.05 V. Similar results were reported by Fernandez *et al.*[18,19] when atomic defects were systematic added under voltammetric conditions on well-ordered surfaces. Nevertheless under alkaline media there is still a lack of data about the GEOR on single crystals electrodes.

Recently, we have published a communication about the electroactivity of Pt(111) towards glycerol electrooxidation in alkaline media.[23] Using FTIR technique we have reported that the GEOR on Pt(111) did not produce substantial CO_{ads} within the potential window studied and insipient CO_2 signal, in contrast with results recorded at acid electrolytes. Clearly, a catalytic process that leads to partial oxidation of the reactant and at high reaction rates might be attractive in electrosynthesis.

Moreover, the above mentioned study was a small part of our interest in comprehends the details on the kinetics and mechanism reaction behavior of platinum catalysis towards glycerol oxidation under potentiostatic conditions. However, we do not know, at present, a systematic investigation into the effect of GEOR in alkaline media on Pt orientated electrodes despite the growing knowledge about the general catalysis of glycerol electrooxidation; although from the viewpoint of density currents at high pH's the catalytic response is highly enhanced[7]. For instance, we are not aware of any previous published FTIR *in situ* studies with Pt(100) and Pt(110) surfaces for glycerol electrooxidation. In this way, herein we employ the *in situ* FTIR technique to monitor the glycerol electrooxidation reaction at low-index Pt(*hkl*) single crystal electrodes and systematically evaluate the influence of crystallographic orientation under potentiostatic in alkaline electrolyte.

2- Experimental

Experiments were carried out at room temperature in a electrochemical glass cell, including a platinum counter-electrode and a reversible hydrogen electrode (RHE) as

reference. Potentials were measured and quoted versus RHE. Test solutions were prepared from NaOH (Merck) using ultrapure water (Milli-Q – 18.2MOhm) and Glycerol (Sigma-Aldrich). An Autolab PGSTAT128N (Metrohm) potentiostat was used to control the electrochemical experiments. To avoid any effect of the Ohmic drop in the measured current, it was always compensated.

The working electrodes employed in this study were platinum bead-type single crystal electrodes prepared from platinum beads according to Clavilier's technique.[24] With exception of Pt(poly)the electrodes, Pt(111), Pt(110) and Pt(100), were oriented, cut and polished from single crystal beads.

Before each experiment, the single crystal electrodes were flame-annealed, cooled down in a reductive atmosphere (H_2 + Ar) and protected with a drop of ultra-pure water before transferring to the electrochemical cell. The typical cyclic voltammograms (CV) in 0.1M NaOH electrolyte are shown in the Fig. 1. The CV's profiles exhibit the typical features of well-ordered Pt single crystals and are in agreement with previous published results.[25,26]

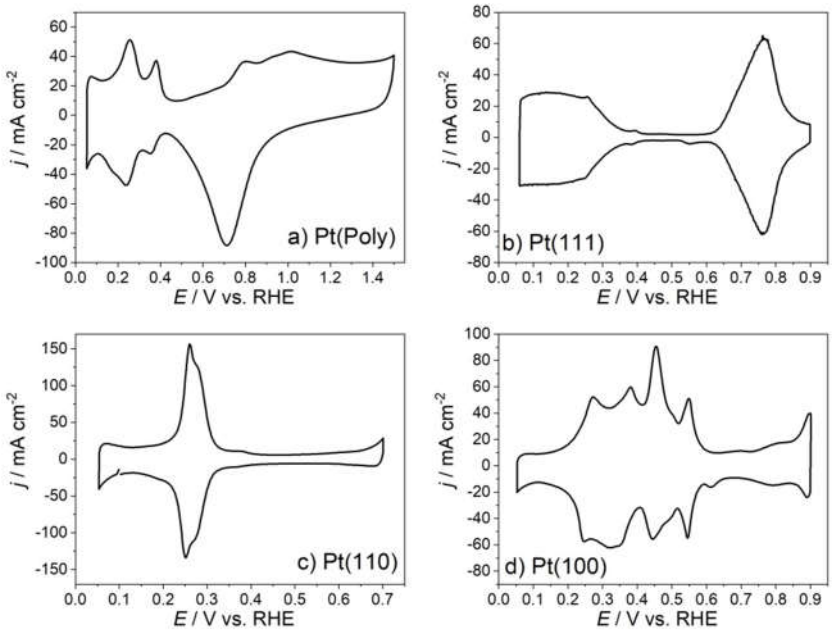

Figure 1: Characteristic platinum cyclic voltammograms in alkaline electrolyte: a) polycrystalline Pt, b) Pt(111), c) Pt(110) and d) Pt(100) in 0.1M NaOH. Scan rate = 50mVs^{-1}

In situ FTIR spectra were acquired using a Nicolet (Model 8700) spectrometer, equipped with mercury-cadmium- telluride (MCT) detector. The spectroelectrochemical cell was coupled in a prismatic CaF_2 window beveled at 60°. The spectra were collected with p-

polarised light with a resolution of 8 cm^{-1}. The spectra are presented as the ratio $-\log(R_2/R_1)$, where R_2 and R_1 are the reflectance values corresponding to the single beam spectra recorded at the sample and reference potentials, respectively.

3 - Results and discussion

3.1-General analysis of voltammetric features of the glycerol oxidation on Pt(h k l) in alkaline media

We begin our electrochemical study by comparing the glycerol CV's on Pt(*hkl*) single crystals model electrodes and polycrystalline platinum (Pt(poly)). The general shape of the polarization curve for GEOR on Pt(*hkl*) in 0.1 mol L^{-1} NaOH are shown in Fig.2. Since the CV profiles for GEOR displays the oxidation currents overlapped in the positive and negative scan – for the sake of clarity – the CV's are presented "unfolded" with respect to the potential axis. It is worth to mention that only the first cycle is presented in Fig.2 due to a large deactivation process upon cycling. This phenomenon will be further discussed along the manuscript.

It is well known that the CV profiles are extremely sensitive to the arrangement of atoms on the electrode surface and the CV behavior is a fair representation of the role of the atoms arrangement on the surface.[27] Avramov-Ivic *et al.*[22] have published a pioneering work of GEOR on Pt(*hkl*) in alkaline solutions. However, the CV profiles displayed present significant differences to that showed in this work. The difference is likely associated with the number of defects on the electrode surface, probably due to the cooling step after thermal treatment, which was carried out in air.

The main characteristic feature that arises from the Fig.2 is that the surface structure is sensitive to glycerol oxidation on Pt electrodes. In fact, such behavior is expected once the literature has an abundant material reporting the catalytic activity characteristics toward the oxidation of small organic molecules; including glycerol,[17,21] methanol,[28] ethanol,[29] ethylene glycol,[29] formic acid,[30] etc. [30,31].

It is important to emphasize that the quality of the single crystal can affect drastically the CV profile, and even small defects on the surface can lead to significant changes in the voltammetric features. Fernandez *et al*. [19] studying the GEOR on Pt(100) in acidic media showed that the presence of randomly distributed defects on the well-ordered (100) surface does not influence significantly the general current signal response but shifts the main

oxidation peak towards more positive potentials. On the other hand, for Pt(111) surface the authors observed a dramatic changes on GEOR response as defects were electrochemically created on the surface.[18] Although it is not the goal of this work, the evaluation of surface defects and its role in GEOR mechanism has its practical importance. The CV of a polycrystalline Pt(poly) is also displayed in Fig 2 in order to help us to understand, even in a qualitatively level, the features of the CV profiles in relation with the arrangement of surface atoms. Detailed analysis of the first CV cycle reveals, as expected, similarities between the GEOR on Pt(poly) and the well-ordered Pt(*hkl*) electrodes. In the positive-going potential scan the potentiodynamic response of the Pt(poly) is composed by one peak with a maximum at 0.81 V with a broad pre-wave contribution between 0.5 to 0.7 V. In spite of the fact that Pt(poly) comprises terrace sites and domains with different length with {111}, {100} and {110} symmetries,[27] its voltammetric profile is the result of the behavior of these sites, which in turn, are related to those observed for the Pt(*hkl*) well-ordered surfaces (See Fig.1). In fact, the contributions of {111} and {110} ordered domains are evident in the CV when we qualitatively compare the presence of the peak ca.0.81 V with the Pt(poly) CV profile. Moreover, the direct correlation from the displayed result between the Pt(poly) and the Pt(*hkl*) surfaces is not straightforward simple because once the most active surface domain starts oxidizing the organic molecule, the solution concentration changes for neighbor domains, which will activate at higher potentials. However, it can be used to understand its behavior and to prepare catalysts with predetermined surface orientation so that activity is maximized.[32]

In our case of study, each of the three single crystal model electrodes exhibits a specific behavior, with significant differences between the CV's. However, the current density responses on the early stages of glycerol oxidation are quite suppressed and the onset reaction does not start below at roughly 0.5 V, regardless the surface orientation. The observed onset potential for the single crystal electrodes studied in this work follows the sequence: Pt(110) < Pt(100) < Pt(111).

It is widely accepted that the onset oxidation potential of small organic molecules is linked to the formation of oxygen-containing species (O-containing) on Pt surface (normally assigned as OH_{ads}) which react with preadsorbed organic species through a Langmuir−Hinshelwood mechanism.[33] One could try to correlate the GEOR onset with potential of zero charge (pzc) of each surface in order to find the initial potential of OH

adsorption and then the explanation of the different onset potential values observed.[25,26] However, such explanation would be an oversimplification of the current system since the double layer is build up by complex adsorbed structures produced from the glycerol interaction with the surface and it would be highly nontrivial to create a finished idea of the whole system. Additionally, the absence of faradaic response within the potential region of 0.05-0.5 V shows that the Pt surface is highly active even at potentials where competitive reactions can take place, e.g. hydrogen adsorption/desorption.[27] In this way, it is more likely that the origin of the onset potential of each surface orientation resides on the nature of these adsorbed species and its bonding to the surface sites, which will depend on their atomic arrangement. Markovic *et al.*[34] showed a direct relation between the onset of the oxidation of ethyleglycol and the formation of O-containing species on Pt single crystals. The role of crystallographic orientation were reported as been stronger in acidic[29] than in alkaline media[35], probably due to formation of different types of adsorbates.

Considering the recent advances in the theoretical description of glycerol adsorption, the studies have shown the complexity of the molecular interaction of glycerol with different sites symmetries, and consequently a complex GEOR mechanism.[36,37] Therefore, due to the molecular structure, it is expected that glycerol molecule decomposition on platinum surface involves several reaction intermediates including products resulting from C-C bond cleavage even at low potentials. This cleavage has been already observed for two-carbon alcohols (ethanol, ethylene glycol) at low potentials.[31,34,38]

As the electrode potential is made more positive the faradaic current related to the GEOR rises and all electrodes responses, except that of Pt(110), display at least one oxidation peak. Among the Pt basal planes, Pt(111) electrode exhibits the highest electroactivity, followed by the Pt(110) and Pt(100). However, this feature is valid only for the first voltammetric cycle. The electrode deactivation under successive potential scans is a typical feature on the Pt electrocatalysis towards the oxidation of small organic molecules, especially in alkaline media.[39] In an recent communication is showed that after the first cycle the Pt(111) electrode has a dramatic deactivation, lowering its electroactivity to about 10% of the highest faradaic response.[23] In acidic media, the GEOR on Pt electrodes follow a similar trend as observed in basic media, in a much less extent.[18–20,40]

From the previous references, it is showed that at low pH values the GEOR proceeds through successive dehydrogenation steps to form single bonded CO as a reaction intermediate (CO_{ads}) at potentials as low as 0.2 V, regardless the surface orientation.[16–18,21] Although the carbon monoxide molecule coordinates strongly to Pt atoms and then could act as surface poison in acidic media, it is oxidized above 0.7 V so that the surface recovers its activity at those potentials. Thus, the strong electrode deactivation over cycles in alkaline media suggests the formation of strong adsorbates different from CO, which are not removed at high potentials and are responsible for the deactivation. In fact, for all studied surfaces the stripping process of the adsorbed residues formed during the course of the GEOR are incomplete within the voltammetric cycle, leading to a buildup of a layer of adsorbed species that cause electrode deactivation over time.

Using *in situ* FTIR we showed that on Pt(111) the formation of adsorbed CO as intermediate during the GEOR is incipient in high pH, and an acyl is the species that remains adsorbed on the surface within the potential window studied.[23] Analogously, the ethanol electrooxidation reaction on Pt electrodes also show high degree of electrode deactivation under high pH.[39,41,42] In addition, when compared with results obtained in acidic solutions, the voltammetric profile of GEOR in alkaline medium is significantly different, showing higher electroactivity, independently of the surface orientation used.[16–21]

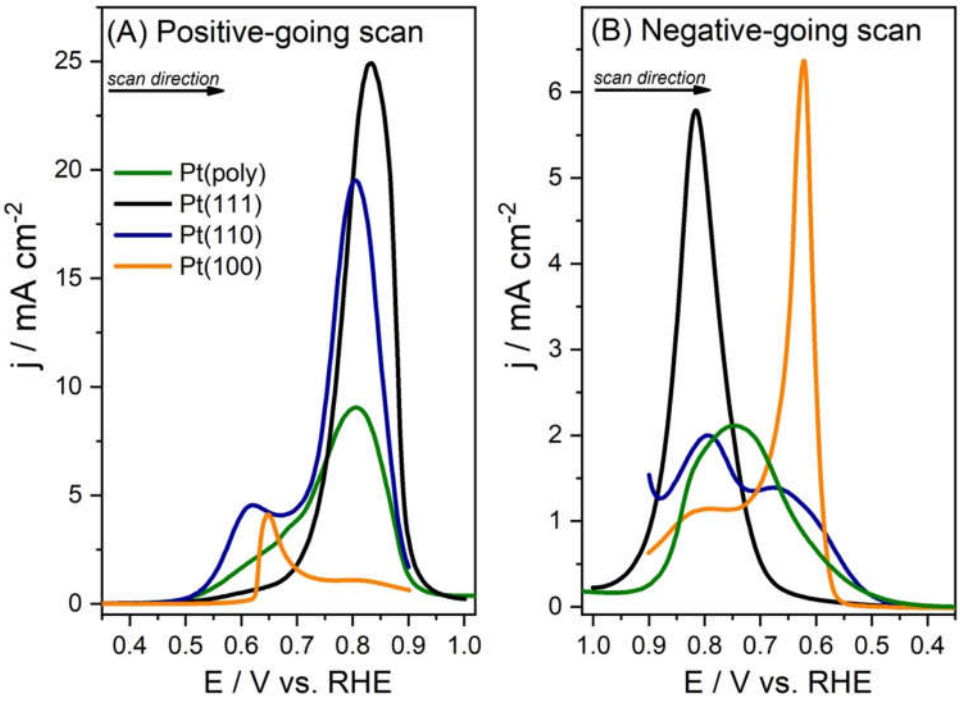

Figure 2: (A) Positive-going scan and (B) negative scan of the 1st cycle of electrooxidation of 0.1 mol L^{-1} glycerol at different surfaces of Pt electrodes in 0.1 mol L^{-1} NaOH. Scan rate of 10 mVs^{-1}. Ohmic drop compensation applied.

Another noticeable characteristic of Fig.2 is the distinct trend of the current densities observed during the negative-going scan. At the beginning of the negative-going scan the surface sites are appreciably occupied, due to the growth of oxide formed at high positive potentials [43] The surface reactivation occurs during the course of the potential in the negative-going direction due to the gradual oxide reduction, cleaning the surface from the oxide. However, the current densities are lower than those measured during the positive-going scan. The extent of the hysteresis between positive and negative-going scans during the GEOR, exhibit mechanistic aspects of the reaction mainly related to the formation of strongly adsorbed intermediates, indicating that during the glycerol oxidation, the formation of these adsorbed residues play a significant role in the GEOR. We could rationalize about the observed hysteresis in terms of stability of the adsorbed intermediates; once they are formed in the positive-going scan, some species remain adsorbed within the potential window during the reverse sweep due to a strong coordination to the surface sites and/or slow oxidation kinetics. Since the deactivation process has been already described on the Pt(111) surface,[23] in the following, a detailed description of the deactivation process on the Pt(100) and Pt(110) will be carried out.

3.2-Glycerol Electrooxidation on Pt(100) and Pt(110) electrodes

Fig. 3 shows the consecutive CV's for the GEOR on both Pt(110) and Pt(100) electrodes. For clarity, positive and negative scan directions have been plotted in different panels. In both cases, The CV features change progressively from the fist to the 20th cycle. The voltammetric profile for the Pt(110) electrode is characterized by the presence of two peaks in the positive scan, centered at ca. 0.65 and 0.79 V, named peak I and II, respectively, with a maximum current density of 20 mA cm^{-2}; while in the reverse scan, these peaks are slightly shifted to more negative potentials. Over cycles, peak I suffers a more accentuated deactivation in contrast to the peak II (see inserts Fig.2A). Thus, after twenty cycles, the intensity of both peaks is very similar. An important feature that should be mentioned is that the currents for the positive scan direction are always higher than those measured in the

preceding negative scan direction, suggesting that desorption of the blocking species may have occurred at potentials close to the hydrogen evolution. In fact in the firsts scan the currents in the positive scan direction are ca. 5-10 times higher than those in the negative direction.

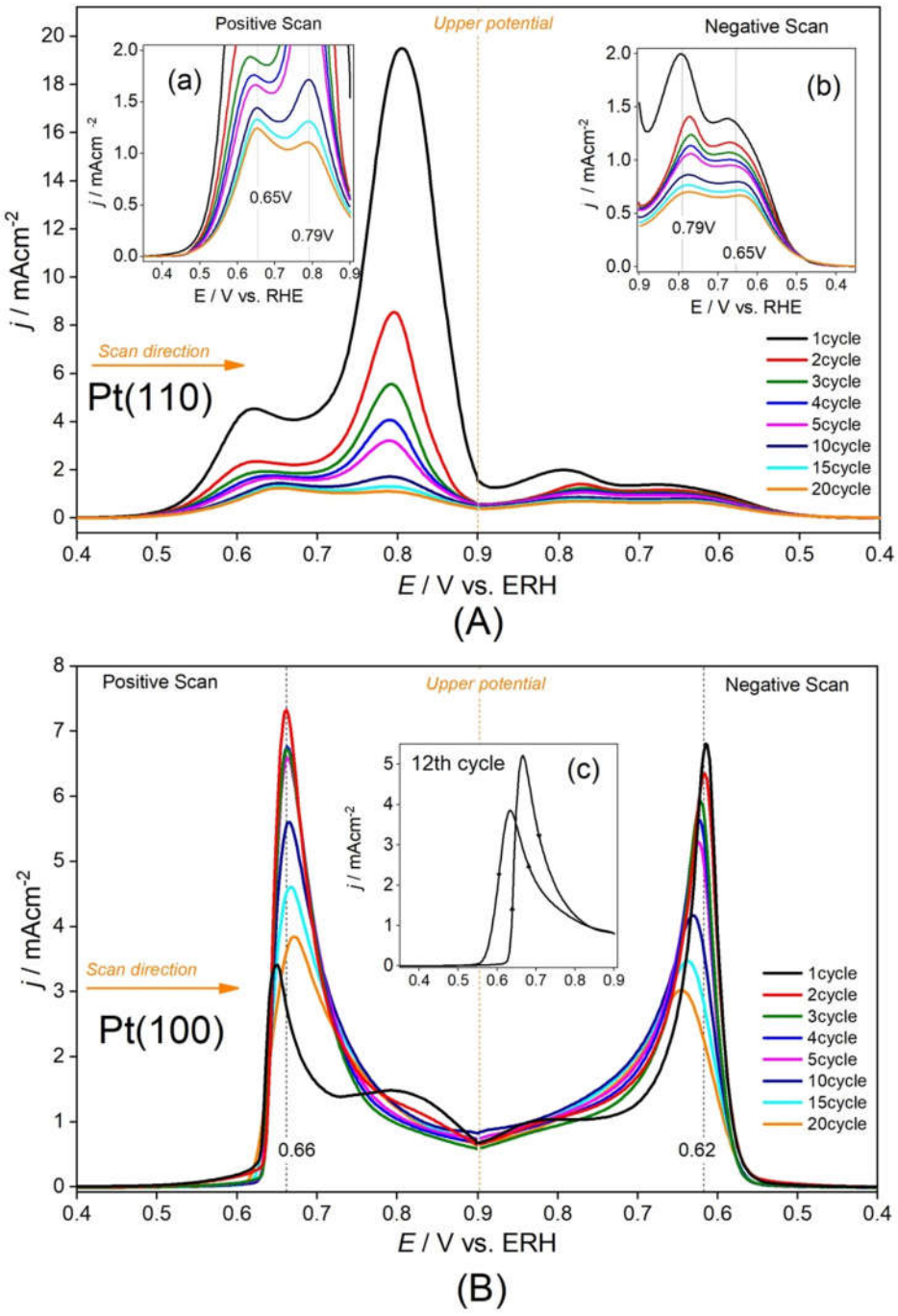

Figure 3: Voltammetric profiles of glycerol electrooxidation on (A) Pt(110) and (B) Pt(100) in 0.1 M glycerol +0.1 M NaOH: scan rate: 10 mV s^{-1} during 20 consecutive cycles.

The insets (a) and (b) show an enlargement of the Pt(110); (c) CV profile of the 12th cycle on Pt(100). Ohmic drop compensation applied.

For the Pt(100) electrode the voltammetric profile is characterized by the presence of only a narrow peak centered at 0.66 and 0.62 V during the positive and negative-going scan, respectively. In this case, the peak at 0.66 V in the first positive scan is small, and after the excursion to 0.9 V, the surface reactivates and the peak at 0.62 V in the negative scan direction has a higher currents. Moreover, there is a hysteresis observed by the shift in the potential region at which currents are recorded. In a general way, from the second to the 20th cycle the changes in the voltammetric profile are not very important, however, the electrode suffers a progressive deactivation over time, but at lesser extent than that observed on two other basal planes. In this case, the currents in the positive scan are only slightly higher than those recorded in the previous negative scan, implying that there is no desorption of blocking species at low potentials. Remarkably, it is the electrode "reactivation" observed only after the first scan, which suggests that the blocking species formed at low potentials in the first scan are different from those formed at high potentials, and the initial blocking species are removed or oxidized at high potentials.

Here a relevant feature about the hysteresis observed in alkaline media, in contrast with those observed in acidic media, deserves additional attention. In low pH's, the hysteresis phenomenon is reported to be associated to formation and adsorption of CO at low potentials. As a surface poison, the CO_{ads} inhibits further glycerol adsorption which diminishes the current density. The CO_{ads} is only stripped off from the surface as the formation of O-containing species is favored with the increase of the potential. As result, at high potentials the produced CO is readily consumed (oxidized to CO_2) and when the potential is reversed, in the negative scan, a higher amount of Pt sites are available for further GEOR, leading to higher electroactivity. Our results in alkaline solutions show that the peak current densities for the basal plane surfaces are characterized by higher values in the positive than the negative-going scans. This remarkable result suggests that the mechanism of glycerol electrooxidation in alkaline electrolyte proceeds in a different form than that reported in acidic media.

3.3-FTIR in situ Experiments of Glycerol Oxidation

In order to obtain more information about the GEOR on Pt(110) and Pt(100) electrodes we performed a FTIR-*in situ* experiments. Fig. 4 shows a series of typical FTIR spectra of the

adsorbates recorded as the potential was externally changed from 0.05 to 0.95 V. The presence of a positive band in Fig. 4 represents to the formation and/or adsorption of species that were not present in the reference spectrum. In this way, potential induced changes in the FTIR signals can be associated with the production/consumption of reaction intermediate during the GEOR, with exception of the band around 1630 cm^{-1} that related to the OH bend vibration mode from the water present in the thin layer.

The potential-dependent FTIR spectra for GEOR is almost featureless until ca. 0.3 V where a band at 2028 cm^{-1} starts to form for the Pt(110) electrode. The wavenumber region between 2100 cm^{-1} and 1800 cm^{-1} are normally assigned to the stretch vibration modes ν(CO) of carbon monoxide of adsorbed on Pt surfaces with different bond geometries.[44] In particular, FTIR features between 2080 and 2000 cm^{-1} are assigned to C≡O stretching mode of the linear-bonded CO adsorbed molecules, CO_L, whence the band here observed at 2028 cm^{-1} is clearly assigned to CO linearly adsorbed on Pt electrode. The presence of the ν(CO) mode is particularly representative of the Pt electrode ability to catalyze the C-C bond scission from glycerol dissociative adsorption. In contrast, on Pt(100) the ν(CO) band is almost indiscernible, however a very small band around 2014 cm^{-1} can be dimly discerned and remains present during the positive and negative-going scan above 0.5 V.

In acidic media, it was reported that single crystal stepped surfaces with (110) steps symmetry favor the C–C bond scission and consequent formation of CO_{ads} during ethanol electrooxidation.[38][45] However, the higher ability to cleavage C-C bond does not imply that the Pt(110) electrodes necessarily present the highest activity for GEOR. Analyzing the voltammograms on Fig. 3 we can observe that after the 10^{th} cycle the density current on Pt(100) is approximately 3 times higher than the Pt(110). It should be kept in mind that the formation of the surface adlayer involves, besides CO_{ads}, other adsorbates from the glycerol molecule, in which the C–C bond remains intact and could act as a poison as well. Additionally, concomitantly with the ν(CO) band, the appearance of the feature at 2340 cm^{-1} assigned to O–C–O asymmetric stretching mode of CO_2 in solution ($\nu(CO_2)$) can be observed. This feature is an indicative that the Pt(110) and Pt(100) electrodes can catalyze the glycerol oxidation reaction to CO_2. However, the presence of the $\nu(CO_2)$ mode is quite informative with regard to the change of the pH in the thin layer configuration. The appearance of the CO_2 band at high potentials can be correlated to the decrease of pH once the carbonate species (CO_3^{-2})

formed after the oxidation of CO are converted into CO_2 due to the depletion of hydroxyl ions from the electrolyte.[46,47]

The analysis of the FTIR spectra during the GEOR is not trivial, because the glycerol molecule can interact with the Pt sites through the oxygen and the carbon resulting on a myriad of possible forms of bonding configuration and molecular geometries, whose vibration spectra corresponds to the range of 1100 -1750 cm^{-1}. Thus, the analysis requires a careful discussion. In the FTIR spectra for both electrodes, two prominent bands at around 1400 cm^{-1} and 1600 cm^{-1} can be observed. The appearance of these features coincides with the faradaic onset of the GEOR as observed in the cyclic voltammograms (Fig.3). i.e. at 0.4 V and 0.5 V on Pt(110) and Pt(100), respectively. At first approximation, they could be attributed to symmetric and asymmetric vibrations of bidentate coordinated carboxylate(ν(COO)),[46–48] produced after the partial oxidation of glycerol in hydroxyacids and keto acids[8,49,50]. The band at 1400-1408 cm^{-1} can be clearly assigned to the symmetric $\nu(OCO)_s$ stretching mode because bands in the same region were observed for other carboxylate such as formate, acetate or citrate and assigned to the bidentate coordinate carboxylate. However, the band at 1580 a 1600 cm^{-1} cannot be attributed to the asymmetric stretching mode because this vibrational mode would be inactive in the FTIR due to the surface selection rule[48,51]. On the other hand, the same band was observed for Pt(111) in the same experimental conditions and the authors assigned the 1585 cm^{-1} band to the C=O stretch mode of acyl intermediate species $\nu(C=O)_{acyl}$ coordinated to the Pt site through the carbon of the carbonyl group (η^1(C)-acyl).[23] Once formed, the $\nu(C=O)_{acyl}$ band remains present during the negative-going scan, suggesting that the acyl specie is the responsible for the electrode deactivation over cycles. The assignment of the band at 1585 cm^{-1} to $\nu(C=O)_{acyl}$ is supported by works conducted in UHV environment.[52–54]

A close inspection of the $\nu(OCO)_s$ mode reveals that a band intensity loss is companied by the appearance of a vibrational feature at 1370 cm^{-1} as the potential increases. This positive band can be assigned to OCO vibrational mode of carbonate specie [46] in solution which is formed at the expense of the adsorbed carboxylate. As discussed earlier, the presence of carbonate signal is an indicative of the oxidation of glycerol to CO_2 product in alkaline media. Concomitantly, the CO_2 band appears and its intensity increases at high potentials, which suggests that is being produced and accumulated in the thin layer at those

potentials. When the scan is reversed and the potential is below 0.6 V, this band diminishes progressively indicating that CO_2 diffuses away from the thin layer and no further CO_2 is formed below this potential.

The spectra also shows additional bands related to the formation/consumption of species at 1628 cm^{-1}, which is present on Pt(100) but absent on Pt(110) surface. It should be highlighted that this band is already visible at potentials as low as 0.1 V. In this wavenumber region two possible vibrational modes can be envisaged and associated to the water bending and C=O stretching of carbonylic groups.[55] Schnaidt *et al.*[16] assigned a band at 1630 cm^{-1} to C=O stretching mode of adsorbed carbonyl species through the C1 carbon, named as glyceroyl. However, under UHV conditions, McManus *et. al.*[52] observed, during thermal desorption of glyceraldehyde on Pt(111), the presence of a band at 1617 cm^{-1} corresponding to coordination of this species to surface through the oxygen of the aldehyde group, namely η^1(O)-aldehyde.

The present results can be rationalized considering the effect of pH equilibrium in the GEOR. It has been shown that the pH plays an important role on the reaction rates of electrooxidation of small organic molecules on several metal catalysts [7,56,57] The following discussion was inspired from the work published by Zope *et.al.*[58] who propose an explanation for the superior activity of Pt and Au nanoparticles at high pH. The main idea is that the glycerol molecule behaves as a very weak acid. At high pH, glycerol undergoes the deprotonation of the alcoholic form to the corresponding alkoxide ($GlyO^-$) via a homogeneous acid-base equilibrium according to:

$$GlyOH_{sol} + OH^-_{sol} \rightleftharpoons GlyO^-_{sol} + H_2O \qquad \text{Equation 1}$$

The concentration of the alkoxide is directly proportional to the pH of the electrochemical system. In our case, and considering the electrochemical environment, the increase of potential can facilitate the alkoxide formation due to the increase of OH^- concentration near the metal/solution interface. Then, the presence of the band around 1630 cm^{-1} can be assigned to presence of the carbonyl group (η^1(O)-aldehyde) coordinated to the surface through the oxygen support the proposition of treating the alkoxide specie as the initial reactive specie of the GEOR in this medium.[9,59,60]

The adsorption of the alkoxide and oxidative removal of one hydrogen from terminal alcohol can yield glyceraldehyde as a reaction intermediate which could in turn reacts in solution though aqueous-phase reaction with OH^- forming glycerate anion, responsible of the band at ca. 1400 cm^{-1}.[58] The behavior of this mode with the electrode potential can be attributed to the consumption of the glycerate, which can act as a precursor for the formation of other adsorbed intermediates and/or reaction products

Alternatively, once adsorbed, the alkoxide can proceed to the dehydrogenation of C-H bond to form the η^1(C)-acyl species as an intermediate giving rise to the band at 1620 cm^{-1}. In the η^1(C)-acyl adsorption geometry, the carbon atom bonds to Pt surface through the carbonyl π- and π*-orbitals with platinum d-orbital in the so-called "back-bonding" interaction, resulting in a strong adsorbed intermediate. This type of strong interaction is also present in the adsorption of CO on the surface, giving rise to the formation of very stable adsorbates. In this case, the $\nu(C{=}O)_{acyl}$ band is observed over a wide potential range and thus the η^1(C)-acyl species can be considered as the poison responsible for the electrode deactivation. Moreover, we suggest that the acyl intermediate is the precursor for the CO_{ads} formation, and consequently one of the possible pathways to the formation of CO_2/ CO_3^{-2} after the C-C bond scission. On the other hand, the observed oxidative C-C bond cleavage in glycerol on Pt(*hkl*) also suggests that the GEOR to CO_2 not necessarily undergoes through η^1(C)-acyl intermediate as indicated by the presence of the ν(OCO) band associated with the $\nu(OCO)_s$ bands, 1370 cm^{-1} and 1400 cm^{-1} respectively. In fact, the latter suggestion indicates that the GEOR on Pt(hkl) occurs mainly through surface intermediates that are weakly coordinated to the surface, for instance from alkoxides, aldehydes or carboxylates which can be further oxidized within the studied potential window. Finally, we expect the mechanistic features discussed in this work and their dependence with surface structure can be used to design new nanostructured materials with desired surface atoms orientations.[14][42] as well as to understand the reaction mechanism of polyols with higher number of carbon atoms.

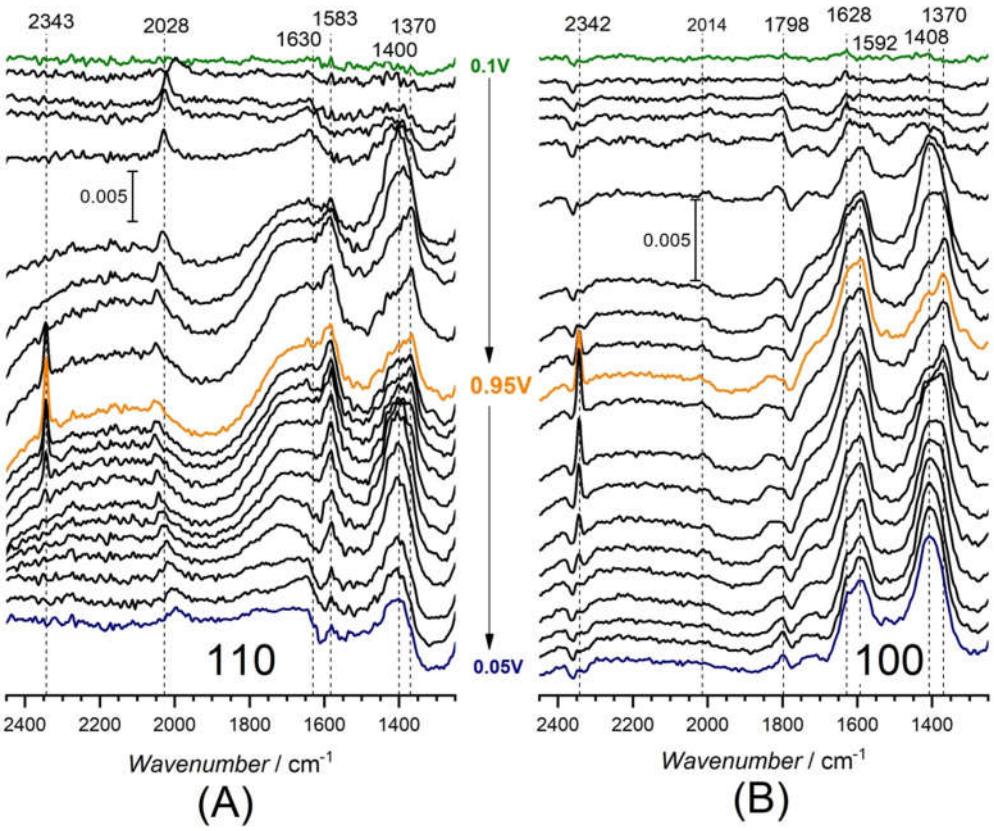

Figure 4. *In situ* FTIR spectra at (A) Pt(110) and (B) Pt(100) in 0.1 molL^{-1} glycerol +0.1 molL^{-1} NaOH as a function of the increasing potential steps from 0.05 to 0.9 V . The reference spectrum was recorded at 0.05 V.

4- Conclusion

Here we have presented, for the first time, some insights of the reaction mechanism and its dependence of surface atoms orientation. Voltammetric profiles and *in situ* FTIR results showed that the glycerol adsorption and electrooxidation at platinum electrodes is a surface sensitive reaction. We have showed clear evidences that the GEOR mechanism takes place through a dehydrogenation reaction (C–H bond cleavage) to form an acyl intermediate as indicated by the $\nu(C{=}O)_{acyl}$ mode, which remains adsorbed even at high potentials and are considered as the responsible to the severe electrode deactivation over cycles. Only the Pt(110) surface revealed ability to break C–C bond at low potentials depicted by the presence of CO band. Conversely, the other basal planes electrodes the CO band was negligible or dimly discerned. Our results have shown that the Pt(*hkl*) electrodes were capable of oxidize glycerol up to carbonate in alkaline electrolyte involving a variety of different intermediates.

5- ACKNOWLEDGMENTS

The authors thank: *Coordenação de Aperfeiçoamento de Pessoal de Nível Superior - CAPES (Brasil)* - Finance Code 001; São Paulo Research Foundation – FAPESP (Brasil): (projects 2013/13749-0 and 2018-10292-2); CNPq – (Brasil) (projects 456758/2014-3 and 474590/2013-5; and J.R.S. scholarship CNPq: 216981/2014-0) and MCINN-FEDER (Spain) project CTQ2016-76221-P.

6- References

[1] R. Ciriminna, C. Della Pina, M. Rossi, M. Pagliaro, *Eur. J. Lipid Sci. Technol.* **2014**, *116*, 1432–1439.
[2] D. T. Johnson, K. A. Taconi, *Environ. Prog.* **2007**, *26*, 338–348.
[3] M. Ayoub, A. Z. Abdullah, *Renew. Sustain. Energy Rev.* **2012**, *16*, 2671–2686.
[4] M. Besson, P. Gallezot, *Catal. Today* **2000**, *57*, 127–141.
[5] Y. Holade, C. Morais, K. Servat, T. W. Napporn, K. B. Kokoh, *Acs Catal.* **2013**, *3*, 2403–2411.
[6] V. L. Oliveira, C. Morais, K. Servat, T. W. Napporn, P. Olivi, K. B. Kokoh, G. Tremiliosi-Filho, *Electrocatalysis* **2015**, *6*, 447–454.
[7] J. F. Gomes, G. Tremiliosi-Filho, *Electrocatalysis* **2011**, *2*, 96–105.
[8] Y. Kwon, K. J. P. Schouten, M. T. M. Koper, *ChemCatChem* **2011**, *3*, 1176–1185.
[9] N. Y. Suzuki, P. V. B. Santiago, T. S. Galhardo, W. A. Carvalho, J. Souza-Garcia, C. A. Angelucci, *J. Electroanal. Chem.* **2016**, *780*, 391–395.
[10] J. F. Gomes, A. C. Garcia, L. H. S. Gasparotto, N. E. de Souza, E. B. Ferreira, C. Pires, G. Tremiliosi-Filho, *Electrochim. Acta* **2014**, *144*, 361–368.
[11] A. Dector, F. M. Cuevas-Muñiz, M. Guerra-Balcázar, L. A. Godínez, J. Ledesma-García, L. G. Arriaga, *Int. J. Hydrogen Energy* **2013**, *38*, 12617–12622.
[12] L. Zhang, A.-J. Wang, J.-J. Feng, X.-Y. Huang, X.-F. Zhang, *ACS Appl. Energy Mater.* **2018**, *1*, 5779–5786.
[13] X.-L. Chen, G.-L. Wen, H. Huang, A.-J. Wang, Z.-G. Wang, J.-J. Feng, *J. Colloid Interface Sci.* **2019**, *540*, 486–494.
[14] Y. Zhou, Y. Shen, J. Xi, *Appl. Catal. B Environ.* **2019**, *245*, 604–612.
[15] Y. Zhou, Y. Shen, J. Piao, *ChemElectroChem* **2018**, *5*, 1636–1643.
[16] J. Schnaidt, M. Heinen, D. Denot, Z. Jusys, R. Jürgen Behm, *J. Electroanal. Chem.* **2011**, *661*, 250–264.
[17] A. C. Garcia, M. J. Kolb, C. van Nierop y Sanchez, J. Vos, Y. Y. Birdja, Y. Kwon, G. Tremiliosi-Filho, M. T. M. Koper, *ACS Catal.* **2016**, *6*, 4491–4500.
[18] P. S. Fernández, P. Tereshchuk, C. A. Angelucci, J. F. Gomes, A. C. Garcia, C. A. Martins, G. A. Camara, M. E. Martins, J. L. F. Da Silva, G. Tremiliosi-Filho, *Phys. Chem. Chem. Phys.* **2016**, *18*, 25582–25591.
[19] P. S. Fernández, J. Fernandes Gomes, C. A. Angelucci, P. Tereshchuk, C. A. Martins, G. A. Camara, M. E. Martins, J. L. F. Da Silva, G. Tremiliosi-Filho, *ACS Catal.* **2015**, *5*, 4227–4236.

[20] P. S. Fernández, C. A. Martins, C. A. Angelucci, J. F. Gomes, G. A. Camara, M. E. Martins, G. Tremiliosi-Filho, *ChemElectroChem* **2015**, *2*, 263–268.
[21] J. F. Gomes, F. B. C. de Paula, L. H. S. Gasparotto, G. Tremiliosi-Filho, *Electrochim. Acta* **2012**, *76*, 88–93.
[22] M. Avramov-Ivic, J.-M. Léger, B. Beden, F. Hahn, C. Lamy, *J. Electroanal. Chem.* **1993**, *351*, 285–297.
[23] R. M. L. M. Sandrini, J. R. Sempionatto, E. Herrero, J. M. Feliu, J. Souza-Garcia, C. A. Angelucci, *Electrochem. commun.* **2018**, *86*, 149–152.
[24] J. Clavilier, R. Faure, G. Guinet, R. Durand, *J. Electroanal. Chem.* **1980**, *107*, 205–209.
[25] R. Rizo, E. Sitta, E. Herrero, V. Climent, J. M. Feliu, *Electrochim. Acta* **2015**, *162*, 138–145.
[26] R. M. Arán-Ais, M. C. Figueiredo, F. J. Vidal-Iglesias, V. Climent, E. Herrero, J. M. Feliu, *Electrochim. Acta* **2011**, *58*, 184–192.
[27] A. Rodes, K. El Achi, M. A. Zamakhchari, J. Clavilier, *J. Electroanal. Chem. Interfacial Electrochem.* **1990**, *284*, 245–253.
[28] T. Iwasita, *Electrochim. Acta* **2002**, *47*, 3663–3674.
[29] J. M. Orts, A. Fernandez-Vega, J. M. Feliu, A. Aldaz, J. Clavilier, *J. Electroanal. Chem. Interfacial Electrochem.* **1990**, *290*, 119–133.
[30] C. A. Angelucci, H. Varela, E. Herrero, J. M. Feliu, *J. Phys. Chem. C* **2009**, *113*, 18835–18841.
[31] R. M. Arán-Ais, E. Herrero, J. M. Feliu, *Electrochem. commun.* **2014**, *45*, 40–43.
[32] C. Busó-Rogero, S. Brimaud, J. Solla-Gullon, F. J. Vidal-Iglesias, E. Herrero, R. J. Behm, J. M. Feliu, *J. Electroanal. Chem.* **2016**, *763*, 116–124.
[33] T. Iwasita, in *Handb. Fuel Cells*, John Wiley & Sons, Ltd, Chichester, UK, **2010**.
[34] V. Del Colle, J. Souza-Garcia, G. Tremiliosi-Filho, E. Herrero, J. M. Feliu, *Phys. Chem. Chem. Phys.* **2011**, *13*, 12163.
[35] N. M. Marković, M. L. Avramov-Ivić, N. S. Marinković, R. R. Adžić, *J. Electroanal. Chem. Interfacial Electrochem.* **1991**, *312*, 115–130.
[36] P. Tereshchuk, A. S. Chaves, J. L. F. Da Silva, *J. Phys. Chem. C* **2014**, *118*, 15251–15259.
[37] M. Valter, M. Busch, B. Wickman, H. Grönbeck, J. Baltrusaitis, A. Hellman, *J. Phys. Chem. C* **2018**, *122*, 10489–10494.
[38] J. Souza-Garcia, E. Herrero, J. M. Feliu, *ChemPhysChem* **2010**, *11*, 1391–1394.
[39] C. Busó-Rogero, E. Herrero, J. M. Feliu, *ChemPhysChem* **2014**, *15*, 2019–2028.
[40] J. F. Gomes, C. A. Martins, M. J. Giz, G. Tremiliosi-Filho, G. A. Camara, *J. Catal.* **2013**, *301*, 154–161.
[41] S. C. S. Lai, M. T. M. Koper, *Phys. Chem. Chem. Phys.* **2009**, *11*, 10446.
[42] C. Busó-Rogero, J. Solla-Gullón, F. J. Vidal-Iglesias, E. Herrero, J. M. Feliu, *J. Solid State Electrochem.* **2016**, *20*, 1095–1106.
[43] B. E. Conway, *Prog. Surf. Sci.* **1995**, *49*, 331–452.
[44] T. Iwasita, F. . C. Nart, *Prog. Surf. Sci.* **1997**, *55*, 271–340.
[45] J. Colmati, F., Tremiliosi-Filho, G., Gonzalez, E., Berna, A., Herrero, E., Feliu, F. Colmati, G. Tremiliosi-Filho, E. R. Gonzalez, A. Berná, E. Herrero, J. M. Feliu, *Phys. Chem. Chem. Phys.* **2009**, *11*, 9114–9123.
[46] P. A. Christensen, S. W. M. Jones, A. Hamnett, *J. Phys. Chem. C* **2012**, *116*, 24681–24689.

[47] T. Iwasita, A. Rodes, E. Pastor, *J. Electroanal. Chem.* **1995**, *383*, 181–189.
[48] M. H. H. Shao, R. R. R. Adzic, *Electrochim. Acta* **2005**, *50*, 2415–2422.
[49] J. F. Gomes, V. L. Oliveira, P. M. P. Pratta, G. Tremiliosi-Filho, *Electrocatalysis* **2015**, *6*, 7–19.
[50] Y. Kwon, M. T. M. Koper, *Anal. Chem.* **2010**, *82*, 5420–5424.
[51] J. L. Davis, M. A. Barteau, *Surf. Sci.* **1991**, *256*, 50–66.
[52] J. L. Davis, M. A. Barteau, *J. Am. Chem. Soc.* **1989**, *111*, 1782–1792.
[53] J. L. Davis, M. A. Barteau, *Surf. Sci.* **1990**, *235*, 235–248.
[54] J. R. McManus, E. Martono, J. M. Vohs, *Catal. Today* **2014**, *237*, 157–165.
[55] J. Schnaidt, M. Heinen, Z. Jusys, R. J. Behm, *J. Phys. Chem. C* **2012**, *116*, 2872–2883.
[56] A. V Tripkovic, K. D. Popovic, B. N. Grgur, B. Blizanac, P. N. Ross, N. M. Markovic, *Electrochim. Acta* **2002**, *47*, 3707–3714.
[57] S. L. Chen, M. Schell, *J. Electroanal. Chem.* **1999**, *478*, 108–117.
[58] B. N. Zope, D. D. Hibbitts, M. Neurock, R. J. Davis, *Science (80-.).* **2010**, *330*, 74–78.
[59] M. S. Ide, R. J. Davis, *Acc. Chem. Res.* **2014**, *47*, 825–833.
[60] Y. Kwon, S. C. S. Lai, P. Rodriguez, M. T. M. Koper, *J. Am. Chem. Soc.* **2011**, *133*, 6914–6917.